

A STUDY OF ATOMIC AND MAGNETIC STRUCTURE OF $\text{La}_{2/3}\text{Pb}_{1/3}\text{Mn}_{1-x}\text{Co}_x\text{O}_3$ USING NEUTRON AND SYNCHROTRON DIFFRACTION METHODS

To Thanh Loan^{1,*}, Bobrikov I. V.², Tran Thi Viet Nga¹, Vu Van Khai³,
Nguyen Huy Sinh⁴

¹*International Training Institute for Materials Science, Hanoi University of Science and Technology, 1 Dai Co Viet, Hai Ba Trung, Hanoi*

²*Frank Laboratory of Neutron Physics, Joint Institute for Nuclear Research, 6 Joliot-Curie, Dubna, Moscow region, Russia*

³*National University of Civil Engineering, 55 Giai Phong Road, Hanoi*

⁴*Hung Yen University of Technology and Education, Dan Tien, Khoai Chau district, Hung Yen*

*Email: totloan@itims.edu.vn

Received: 11 August 2014, Accepted for publication: 29 August 2015

ABSTRACT

The samples with nominal composition of $\text{La}_{2/3}\text{Pb}_{1/3}\text{Mn}_{1-x}\text{Co}_x\text{O}_3$ ($x = 0, 0.15, 0.20$ and 0.25) were prepared by standard solid-state reaction method. Atomic and magnetic structures of the samples have been studied by neutron and synchrotron diffraction. The obtained results showed that, in wide temperature range (8-300 K) all investigated compounds are described by slightly distorted perovskite like structure with rhombohedral symmetry (sp. gr. $R-3c$). The lattice parameters and bond distances Mn/Co–O are typical of rhombohedral manganites. Type of magnetic ordering doesn't depend on doping level of Co: it is ferromagnetic at low temperature with average ordered value of magnetic moment in B-sites of about $3.5 \mu_B$ at $T < 20$ K. In the compound with $x = 0.15$ there exist two crystal phases with the same symmetry but different stoichiometry. Only negligible changes of samples microstructure with composition were observed.

Keywords: Perovskite, atomic structure, magnetic structure, neutron diffraction, synchrotron diffraction.

1. INTRODUCTION

Mixed magnetic oxides of manganese with the perovskite structure have been attracting special experimental and theoretical attention for long time due to their large variety of physical phenomena and diverse practical applications. Since the discovery of CMR effect in manganites [1], the compounds with formula $\text{RE}_{1-x}\text{A}_x\text{MnO}_3$ (RE – trivalent rare earth viz. La, Sm, Pr etc. and A – divalent alkali metal viz. Ca, Sr, Ba etc.) have been widely studied, many of

which have interesting properties. In the family of CMR manganites, the materials doped with Pb are very interesting, because they have rather high T_C and the significant magnetoresistance is observed at room temperature. As found in references, ferromagnetic phase transition temperature of the compound $\text{La}_{0.67}\text{Pb}_{0.33}\text{MnO}_3$ ($T_C \approx 340$ K [2]) is significantly higher than room temperature.

Among divalent cations, Pb^{2+} occupies a special position due to its large ionic radius ($r_{\text{Pb}} = 1.63$ Å, whereas for example $r_{\text{Ca}} = 1.48$ Å), its electrons often form a so-called lone pair, which can lead to strong distortion of structure and displacement of Pb^{2+} ion from the symmetric position. Such phenomenon was observed in structure of PbVO_3 [3]. There is not much research on Pb-doped manganites because of technological difficulties in samples synthesis due to low melting temperature and dissociation of lead oxides. The effect of Pb doping on magnetic and transport properties of $\text{La}_{1-x}\text{Pb}_x\text{MnO}_3$ was studied [2, 4]. Some structural data of Pb-doped manganites was presented in the review [5].

Recently, there have been some studies on Pb-doped manganites with simultaneous substitution for Mn by other transition-metal ions, mostly by Co, radius of which is close to Mn radius. Information on magnetization, magnetic susceptibility, electrical resistivity and atomic structure performed X-ray analysis of composition $(\text{La}_{0.67}\text{Pb}_{0.33})(\text{Mn}_{1-x}\text{Co}_x)\text{O}_3$ (with x from 0 to 0.15) have been published [6, 7]. In the compounds, magnetic characteristics such as the Curie temperature, the effective magnetic moment and the saturated magnetization decrease with increasing Co doping. The similar results were observed with substitution for Mn by other metals (Ni, Fe, Ag) [8, 9].

However up to now, there is no neutron structural study of the compound $(\text{LaPb})(\text{MnCo})\text{O}_3$. Accordingly, there is no information about the ordered magnetic moment and influence of lead and cobalt on the atomic structure of the compound. In this work we present the results of synchrotron and neutron structural studies of the $\text{La}_{2/3}\text{Pb}_{1/3}\text{Mn}_{1-x}\text{Co}_x\text{O}_3$ compound (LPMCO- x) with x from 0 to 0.25 to provide precise data on its atomic and magnetic structure.

2. EXPERIMENTAL

2.1. Sample preparation

The samples with nominal composition of $\text{La}_{2/3}\text{Pb}_{1/3}\text{Mn}_{1-x}\text{Co}_x\text{O}_3$ ($x = 0, 0.15, 0.2$ and 0.25) were prepared by standard solid-state reaction method [10]. Stoichiometric amounts of La_2O_3 , PbO , MnO and Co_2O_3 powder were mixed, ground, pressed into pellets and calcined at 600 °C for 12 h. The samples were then cooled down to room temperature. The pellets were remixed and pressed into pellets again, then sintered at 1000 °C for 10 h and calcined again at 1150 °C for 24 h, cooled down to 650 °C for 12 h, and after that cooled down to room temperature in air.

2.2. Data collection and processing

Synchrotron powder diffraction (SPD) experiments were done at the 01C2 beam line of the synchrotron source NSRRC (Taiwan) with wavelength $\lambda = 0.4959$ Å for $x = 0, 0.2$ and 0.25 . The diffraction patterns were measured in a wide temperature range from 8 K to room temperature. Fig. 1a shows the synchrotron diffraction patterns of the LPMCO- x ($x = 0, 0.2$ and

0.25) samples measured at room temperature. And SPD patterns of the sample LPMCO-0.2 measured at different temperature from 8 K to 300 K are presented in Fig. 1b.

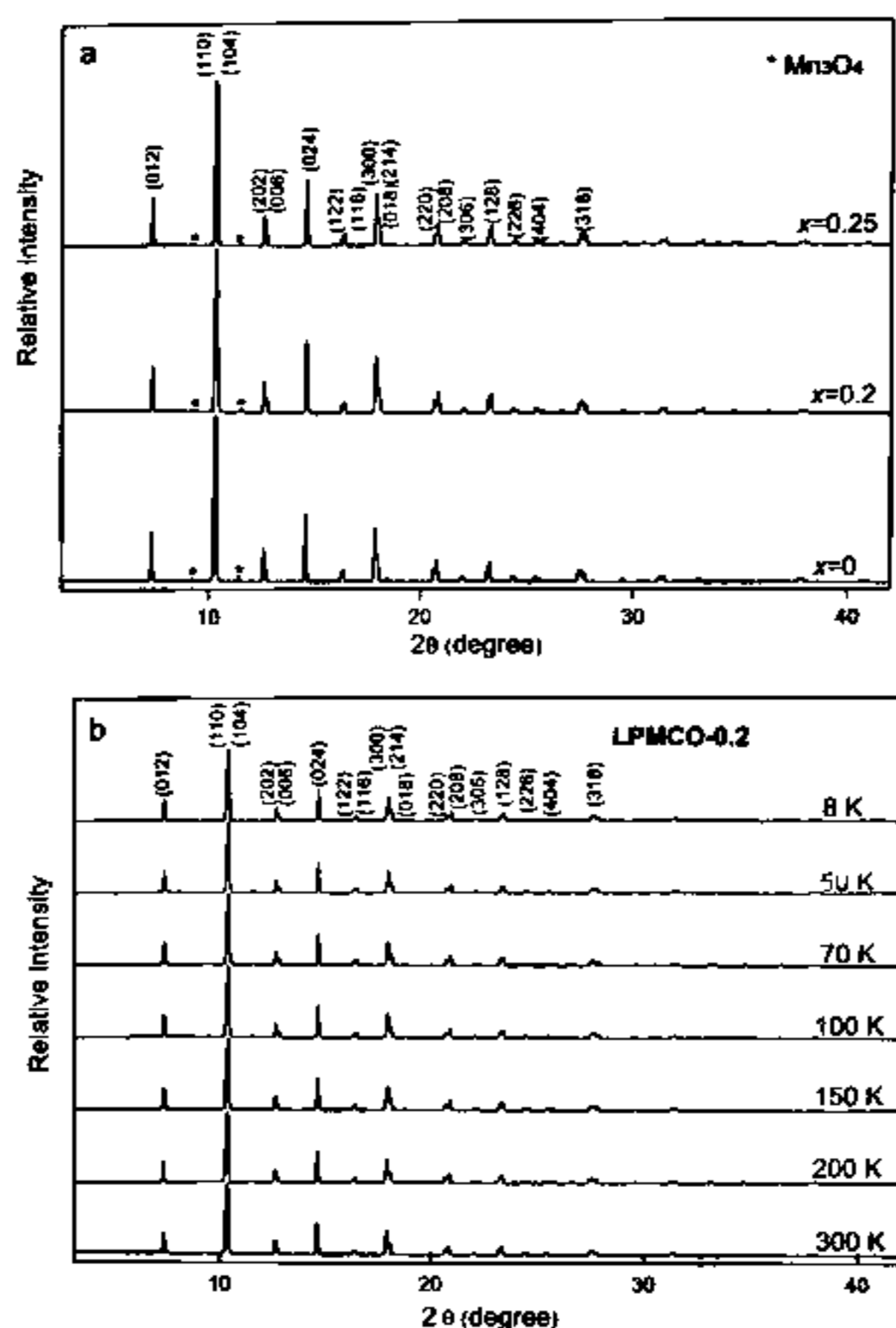


Figure 1. SPD patterns of the LPMCO- x ($x = 0, 0.2$ and 0.25) samples measured at room temperature (a). SPD patterns of the sample LPMCO-0.2 collected at different temperature (b).

Neutron powder diffraction (NPD) experiments were carried out at pulsed reactor IBR-2, Frank laboratory of neutron physics, JINR (Russia). For the compositions $x = 0.15$ and 0.25 the data was obtained on high resolution Fourier diffractometer (HRFD) at room temperature to refine the atomic structure. NPD patterns of the samples are shown in Fig. 2a. For the compositions $x = 0.2$ and 0.25 measurements were performed on diffractometer DN-12 in the wide temperature range (27 K to room temperature) to determine the magnetic structure. Fig. 2b shows the NPD spectra of the sample LPMCO-0.25 measured at different temperature. Both diffractometers use a wide range wavelength and the time of flight method (TOF) for the spectrum scanning.

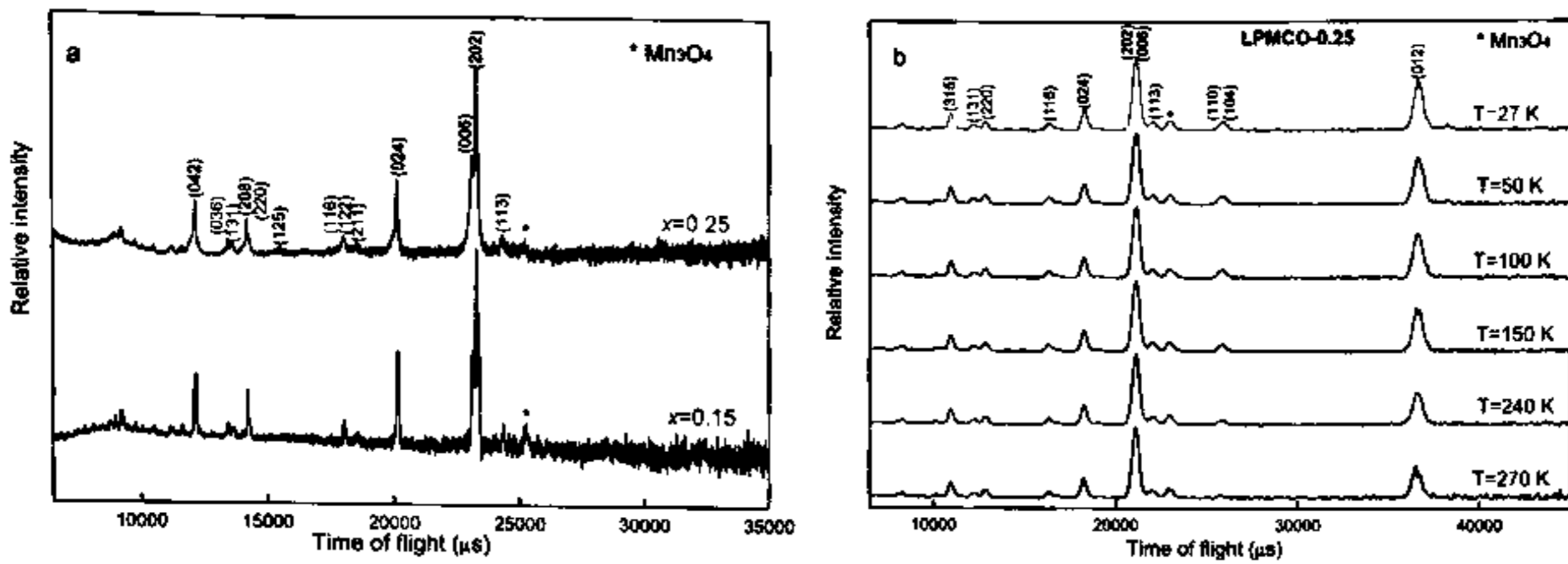


Figure 2. Neutron diffraction patterns of the LPMCO- x ($x = 0.15$ and 0.25) samples measured at room temperature (a). Neutron diffraction patterns of the sample LPMCO-0.25 collected at different temperature (b).

The data analysis was carried out using the Rietveld method with the help of the Fullprof [11] and MRIA [12] programs. The Bragg diffraction peaks were modeled by pseudo-Voigt distribution function which is a sum of Gaussian and Lorentzian functions [13]. A standard of silicon was used to determine instrumental resolution function of the synchrotron diffractometer. Instrumental resolution function of the neutron diffractometers was identified by using a vanadium standard. The refinement fitting quality was checked by goodness of fit (χ^2) and weighted profile R -factor (R_{wp}) [14], which are given in Table 1 and Table 2 for SPD and NPD analysis, respectively. The examples of the synchrotron and neutron diffraction patterns and their refinements are shown in Fig. 3.

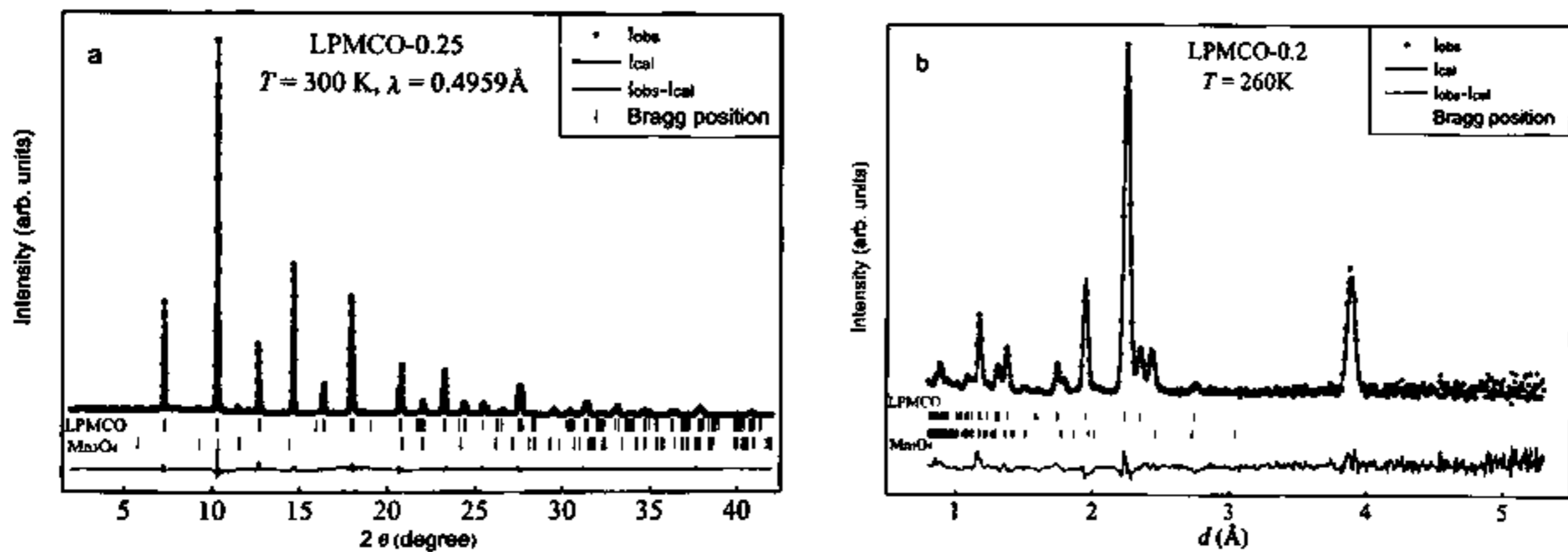


Figure 3. Examples of the Rietveld refinement pattern and diffraction plot of the synchrotron diffraction (a) and the neutron diffraction data (b). The experimental points as well as calculated and difference functions are indicated. The upper row of dashes indicates Bragg positions of LPMCO phase, the lower row – Bragg positions of Mn_3O_4 .

3. RESULTS AND DISCUSSION

3.1. Crystal structure and microstructure

The crystal structure of all the composition LPMCO- x with x from 0 to 0.25 at all temperature (from 8 to 300 K) is well refined in the rhombohedral space group $R\bar{3}c$ with atoms

in positions La/Pb in $6a$ ($1/4, 1/4, 1/4$), Mn/Co in $6b$ ($0, 0, 0$) and O in $18e$ ($x+1/4, -x+1/4, 1/4$). It was found that the samples contain impurity Mn_3O_4 . The concentration of Mn_3O_4 is different in different compositions and given in Table 1.

Table 1. The SPD refinement results: lattice parameters (a, α), unit cell volume (V), atomic coordinates, thermal parameters (B_{iso}), bond lengths (Mn/Co)-O ($d_{(Mn/Co)}$), (La/Pb)-O ($d_{(La/Pb)}$) and refinement fitting quality (χ^2, R_{wp}). Statistical errors are indicated in the last significant digit.

x	0	0.2	0.25
a (b, c), Å	5.4977 (1)	5.4847(1)	5.4871(1)
α (β, γ), °	60.41(1)	60.49(1)	60.40(1)
$V, \text{Å}^3$	118.59(1)	117.97(1)	117.87(2)
$x(O)$	0.458(1)	0.457(1)	0.458(2)
$B_{iso}(La/Pb), \text{Å}^2$	1.69(1)	1.64(1)	1.54(2)
$B_{iso}(Mn/Co), \text{Å}^2$	1.17(2)	0.92(2)	1.14 (4)
$B_{iso}(O), \text{Å}^2$	1.8(1)	1.9(1)	2.0(2)
$d_{(Mn/Co)-O}, \text{Å}$	1.964(4)	1.961(3)	1.959(5)
$d_{(La/Pb)-O}, \text{Å}$	2.762(4)	2.758(3)	2.757(6)
Concentration of Mn_3O_4 , %	5.68	4.74	4.07
R_{wp} , %	8.74	8.11	14.9
χ^2	0.618	2.01	1.21

The structural parameters obtained from synchrotron and neutron diffraction data at room temperature including lattice parameters, unit cell volume, atomic coordinates, thermal parameters, bond lengths (Mn/Co)-O and (La/Pb)-O are listed in Table 1 and Table 2, respectively. As seen in the Table 1 the errors of the metal-oxygen bond length are quite large ($\sim 5 \cdot 10^{-3}$) due to scattering properties of synchrotron X-ray diffraction. The synchrotron are scattered by electrons, thus the atomic scattering factor increases with the atomic number. The intensities of diffraction peaks are dominated by contribution of heavy atoms and hence it makes difficulty in position determination of light elements (hydrogen, oxygen, etc.). But the lattice parameters as well as microstructure parameters were determined precisely due to high resolution and powerful source of synchrotron radiation.

Table 2. The NPD refinement results: lattice parameters (a, α), unit cell volume (V), atomic coordinates, thermal parameters (B_{iso}), bond lengths (Mn/Co)-O ($d_{(Mn/Co)}$), (La/Pb)-O ($d_{(La/Pb)}$) and refinement fitting quality (χ^2, R_{wp}). Statistical errors are indicated in the last significant digit.

x	0.15	0.2	0.25
Diffraction	HRFD	DN-12	DN-12
a (b, c), Å	5.4840(1)	5.4847	5.4871
α (β, γ), °	60.30(0)	60.49	60.40
$V, \text{Å}^3$	117.40(1)	117.97	117.87
$x(O)$	0.5352(4)	0.4511(13)	0.4597(4)
$B_{iso}(La/Pb), \text{Å}^2$	0.4	0.4	0.4
$B_{iso}(Mn/Co), \text{Å}^2$	0.4	0.4	0.4
$B_{iso}(O), \text{Å}^2$	2	0.8	2

$d_{(\text{Mn/Co})-\text{O}}, \text{ \AA}$	1.952(1)	1.965(3)	1.962(1)
$d_{(\text{La/Pb})-\text{O}}, \text{ \AA}$	2.752(1)	2.761(3)	2.756(1)
Concentration of Mn_3O_4 , %	9.65	4.74	4.07
R_{wp} , %	8.23	16.4	3.26
χ^2	1.14	2.93	2.96

The temperature dependences of lattice parameters and microstructure parameters of the compositions with $x = 0, 0.2$ and 0.25 are presented in Fig. 4. Angle α is typical for manganite, decreases with increasing temperature, which indicates a possible transition to the cubic phase with increasing temperature wherein $\alpha = 60^\circ$. The parameters of microstructure including the average size of coherent scattering blocks L and the lattice microstrain σ , were obtained by analysis of the peak broadening. In our work the microstructure parameters were determined on applying Rietveld method using Fullprof program with condition that instrumental resolution function was provided. It can be seen that the average size of coherent scattering region and the magnitude of the lattice microstrain do not depend on temperature and increase with increasing Co concentration. The substitution of Co for Mn leads to a structure disorder of the samples and thus the lattice microstrain increases.

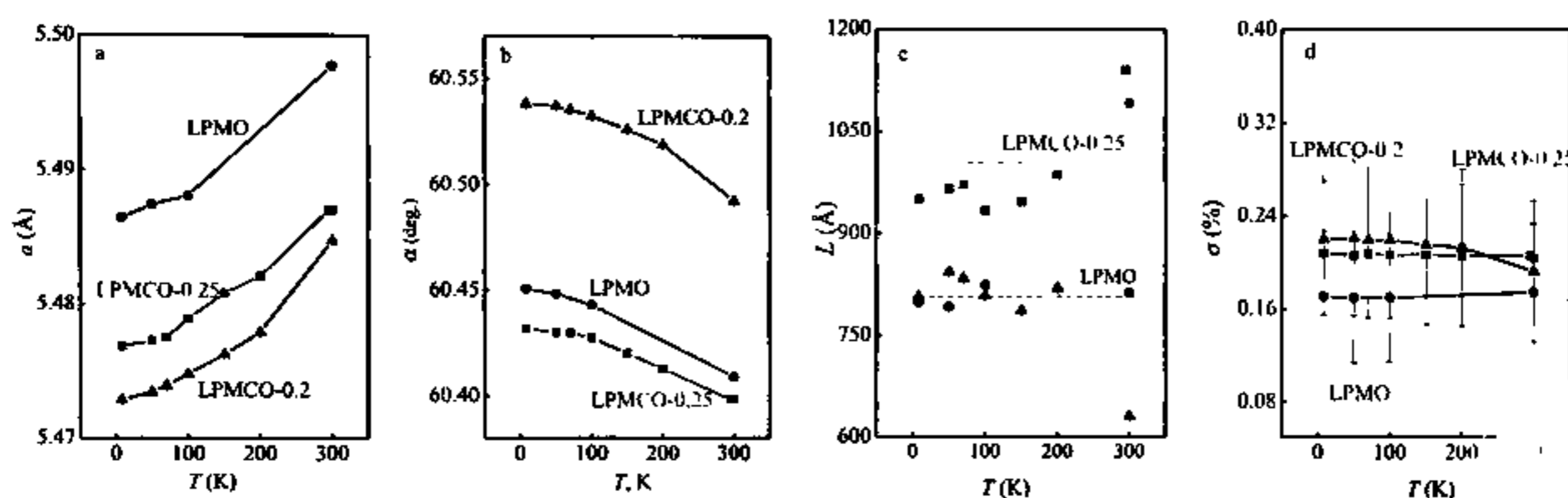


Figure 4. Temperature dependence of lattice parameters (a and b) and microstructural parameters (c and d) of the compound $\text{La}_{2/3}\text{Pb}_{1/3}\text{Mn}_{1-x}\text{Co}_x\text{O}_3$.

The position of oxygen atom for the sample LPMCO- x with $x = 0.15, 0.2$ and 0.25 was determined from neutron diffraction data obtained at neutron diffractometers HRFD and DN-12. As microstructure parameters, bond length Mn/Co-O is identical and weakly depends on temperature (as seen in Fig. 5a), which indicates the absence of structural phase transition in the samples LPMCO- x .

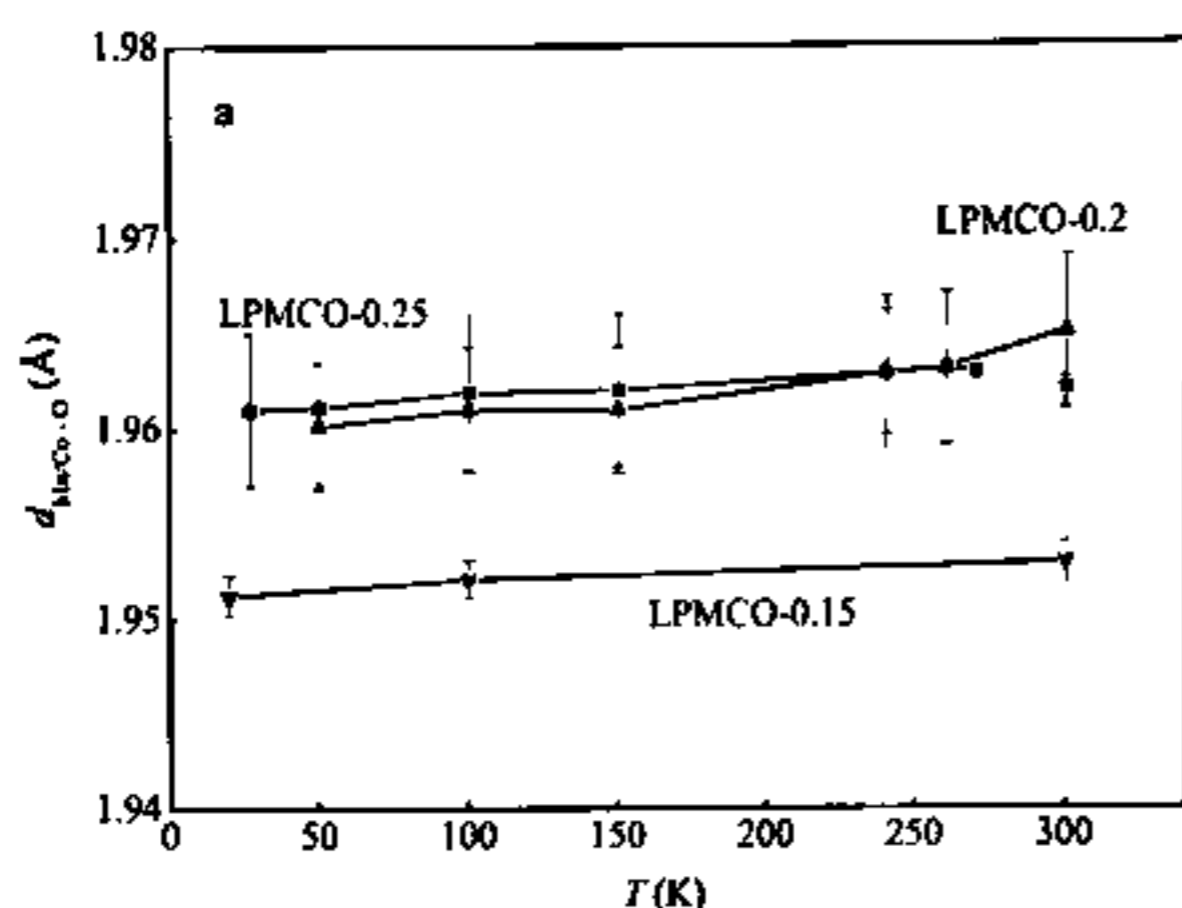


Figure 5a. Temperature dependence of bond length Mn/Co–O for the samples with $x = 0.15, 0.2$ and 0.25 . Data of the samples $x = 0.2$ and 0.25 was collected on DN-12. The data of the samples $x = 0.15$ and $x = 0.25$ at $T = 300$ K was collected on HRFD.

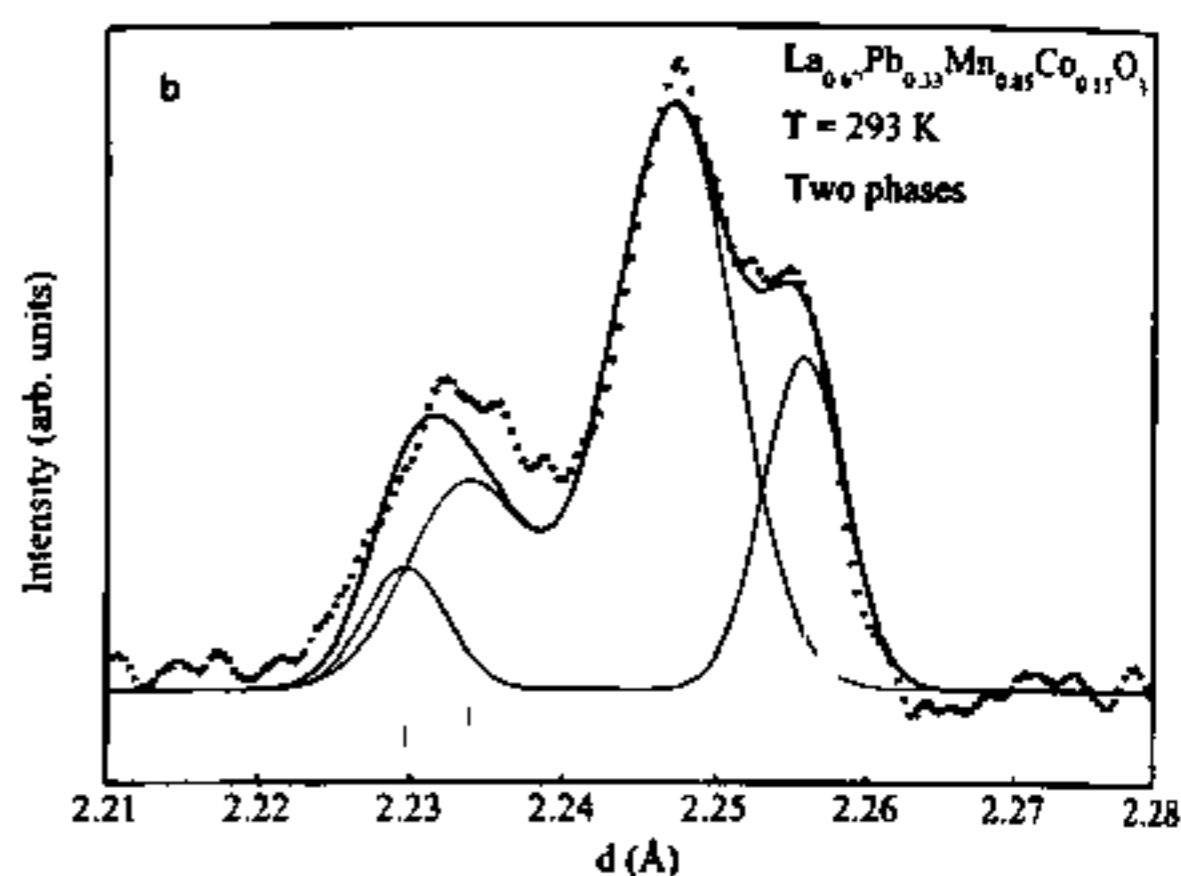


Figure 5b. A plot of the diffraction spectrum measured on HRFD. Experimental point, calculated intensities of two phases and their amount are shown.

In our previous work, electrical resistivity of the samples was investigated [15]. The results showed that the metal-insulator transition temperature decreases with increasing Co content, which is very good agreement with that reported by Gritzner G. et al. [7]. But for the LPMCO-0.15 sample, metal-insulator transition temperature is very low and electrical resistivity is very high compared with other LPMCO- x samples. In order to clarify the nature of the resistivity change in the LPMCO-0.15 sample, NPD data of the compositions $x = 0.15$ and 0.25 were collected on high resolution Fourier diffractometer (HRFD) at room temperature (Fig. 2a). In the diffraction spectrum of the LPMCO-0.15 sample, peak splitting was observed. The refinement result shows (as presented in Fig. 5b) that the sample contains two phases. Both phases are rhombohedral space group $R\bar{3}c$ with different unit cell parameters ($a = 5.4840 \text{ \AA}$, $\alpha = 60.30^\circ$ for the first phase and $a = 5.4858 \text{ \AA}$, $\alpha = 60.58^\circ$ for the second). Ratios of the phases in the sample are 60 % and 40 %, respectively. Mn/Co ratio of the first phase is equal to 85/15, while Mn/Co ratio of the second phase is 85/12. This phase separation was observed only in the sample LPMCO-0.15 and can be related to sample fabrication conditions. The phase separation observed in the LPMCO-0.15 sample is structural reason, which leads to its resistivity change.

3.2. Magnetic structure

Magnetic properties of LPMCO- x materials have been studied by various workers [7, 16]. Their results indicated that the Curie temperature, the effective magnetic moment and the saturated magnetization decrease with increasing Co content. The obtained results were explained mainly due to the double-exchange (DE) that arises from the ratio of Mn^{3+} to Mn^{4+} . Substitution of Co^{3+} for Mn^{3+} leads a depletion of the $\text{Mn}^{3+}/\text{Mn}^{4+}$ ratio, the double-exchange is suppressed resulting in the reduction of ferromagnetism.

The present work aims to identify the magnetic ordering type (magnetic structure) and the value of magnetic moment of LPMCO- x compounds at low temperature. Magnetic structure of the samples was determined from neutron diffraction experiments due to the interaction between magnetic moment of neutron and the magnetic moment of the atoms. In this case the intensity of the diffraction peaks related to atomic order (“nuclear” peaks) appears additional

contribution at low temperature as seen in the Fig. 6a, which indicates that the samples exhibit ferromagnetic (FM) ordering of the Mn and Co spins. No sign of antiferromagnetic ordering was found.

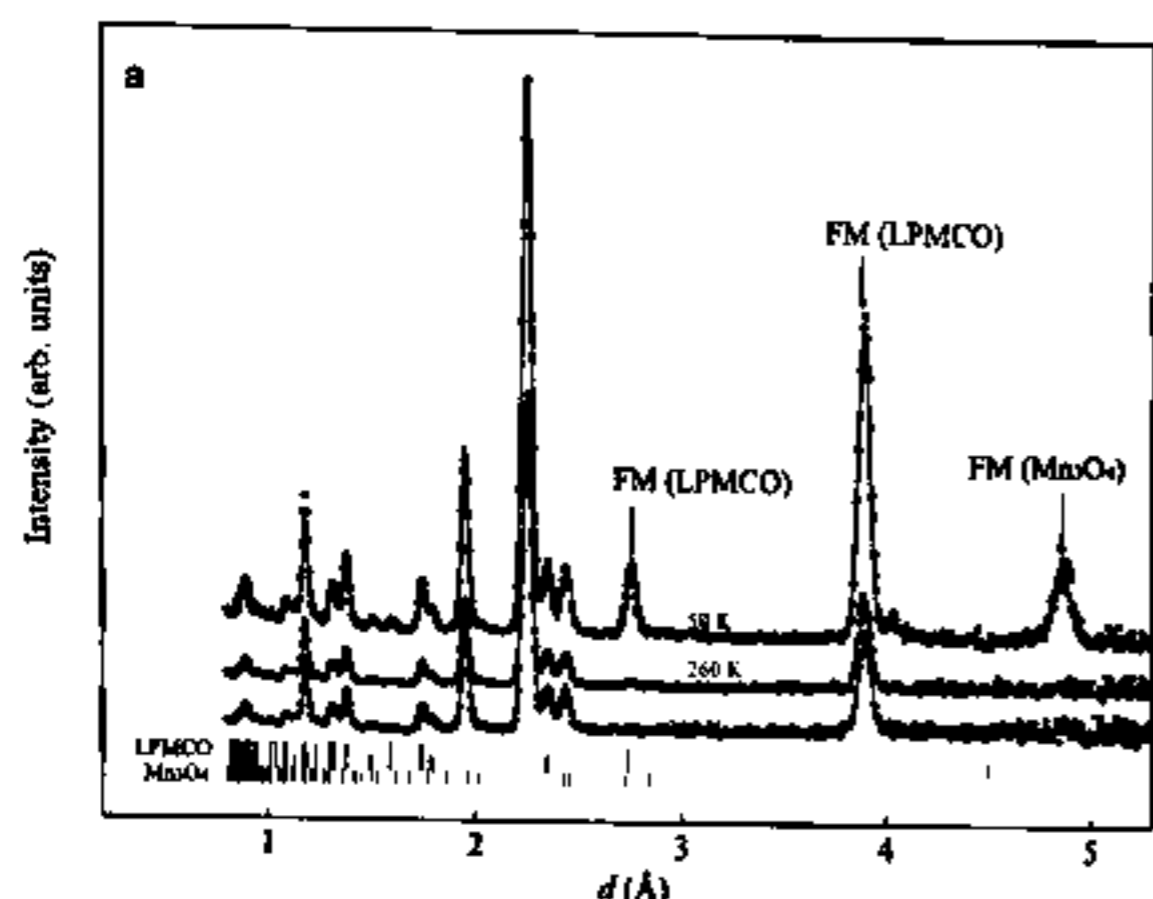


Figure 6a. Neutron diffraction pattern of $\text{La}_{2/3}\text{Pb}_{1/3}\text{Mn}_{0.8}\text{Co}_{0.2}\text{O}_3$ obtained at different temperature $T = 50 \text{ K}$, 260 K and 300 K .

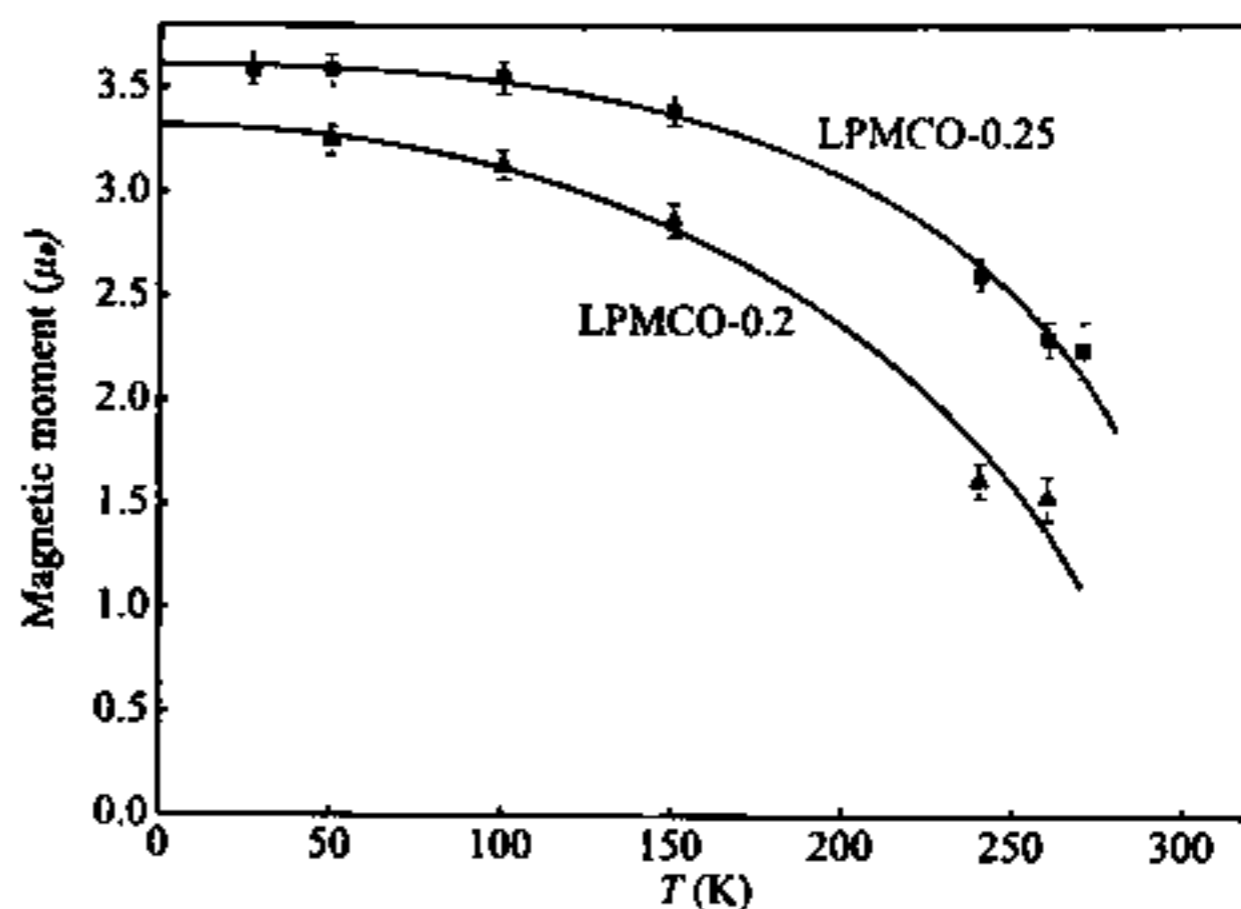


Figure 6b. The temperature dependence of the average magnetic moment of the samples $x = 0.2$ and 0.25 .

The values of the magnetic moments of the compositions with $x = 0.2$ and 0.25 were determined based on the data collected on DN-12 at low temperature ($\leq 270 \text{ K}$). Manganese and cobalt atoms occupy at the same position, therefore only the average magnetic moment of the position was calculated. The temperature dependencies of the refined average magnetic moment are given in Fig. 6b. The lines in Fig. 6b are the fits to the phenomenological formula $\mu(T) = \mu(0)[1 - (T/T_C)^\alpha]^\beta$, which matches well to experimental $\mu(T)$ at temperature T . According to this formula, both magnetic moment at 0 K ($\mu(0)$) and Curie temperature (T_C) can be refined. But as the main aim of this study mentioned above, the experimental points concentrate at low temperature region. Hence the phenomenological formula gives correct values of $\mu(0)$ only. The magnetic moments at 0 K determined from the fit to the formula are $\mu_{\text{Mn/Co}}(0) = (3.32 \pm 0.17) \mu_B$ for $x = 0.2$ and $\mu_{\text{Mn/Co}}(0) = (3.64 \pm 0.11) \mu_B$ for $x = 0.25$, which are close to the magnetic moment value of Mn^{3+} in the parent LaMnO_3 compound. Magnetic moment of Mn^{3+} in LaMnO_3 revealed by neutron diffraction study is equal to $3.5 \mu_B$ [17]. However, it can be seen that $\mu(0)$ increases slightly from $\mu(0) = 3.32$ to $\mu(0) = 3.64$ with increasing Co content from 0.2 to 0.25 , which can be explained due to the change in the Co^{3+} spin state. There are three possible spin state for Co^{3+} ions: low-spin (LS) state ($t^6_{2g}e^0_g$, $S = 0$, $\mu_{\text{eff}} = 0$), intermediate-spin (IS) state ($t^5_{2g}e^1_g$, $S = 1$, $\mu_{\text{eff}} = 2.83 \mu_B$) and high-spin (HS) state ($t^4_{2g}e^2_g$, $S = 0$, $\mu_{\text{eff}} = 4.9 \mu_B$) [18]. In the sample LPMCO-0.2, Co^{3+} ions are mostly in LS and IS states and therefore, magnetic moment in B-site is reduced in comparison to the magnetic moment value of Mn^{3+} in the parent LaMnO_3 compound. For the sample LPMCO-0.25, the presence of HS Co^{3+} ions lead to the increase of magnetic moment in B-site.

4. CONCLUSIONS

The atomic structure, microstructure and magnetic structure of $(\text{La}_{2/3}\text{Pb}_{1/3})(\text{Mn}_{1-x}\text{Co}_x)\text{O}_3$ samples (with $x = 0, 0.15, 0.2$ and 0.25) have been investigated systematically by means of synchrotron and neutron powder diffraction. The crystal structure symmetry of the compounds was confirmed to be rhombohedral (sp. gp. $R-3c$) in the whole investigated range of x . No

evidence of structural phase transition in the samples in the temperature range from ~10 K to room temperature is observed. A phase separation was identified in the sample with $x = 0.15$. It was confirmed that at low temperature LPMCO- x has ferromagnetic ordering type. The average values of magnetic moment in B-site were determined to be close to the magnetic moment value of Mn^{3+} in the parent $LaMnO_3$ compound and slightly change due to the change in spin state of Co^{3+} ions.

REFERENCES

1. Jin S., Tiefel T. H., McCormack M., Fastnacht R. A., Ramesh R., and Chen L. H. – Thousandfold change in resistivity in magnetoresistive La-Ca-Mn-O films, *Science* **264** (1994) 413-415.
2. Peles A., Kunkel H. P., Zhou X. Z., and Williams G. – Field-dependent magnetic and transport properties and anisotropic magnetoresistance in ceramic $La_{0.67}Pb_{0.33}MnO_3$, *J. Phys.: Condens. Matter* **11** (1999) 8111-8130.
3. Shpanchenko R. V., Chernaya V. V., Tsirlin A. A., Chizhov P. S., Sklovsky D. E., Antipov E. V., Khlybov E. P., Pomjakushin V., Balagurov A. M., Medvedeva J. E., Kaul E. E., and Geibel C. – Synthesis, structure, and properties of new perovskite $PbVO_3$, *Chem. Mater.* **16** (2004) 3267-3273.
4. Singh R. J., and Sharma P. K. – Magnetic order and electrical resistance in manganites, *Indian J. of Pure & Applied Physics* **43** (2005) 273-278.
5. Salamon M. B., and Jaime M. – The physics and manganites: structure and transport, *Rev. Mod. Phys.* **73** (2001) 583-627.
6. Mihalik M., Kavecansky V., Matas S., Zentkova M., Ammer J., Kellner K., and Gritzner G. – Magnetic and Transport properties of $La_{0.67}Pb_{0.33}(Mn_{1-x}Co_x)O_3$, *Acta Physica Polonica A* **113** (2008) 251-254.
7. Gritzner G., Ammer J., Kellner K., Kavecansky V., Mihalik M., Matas S., and Zentkova M. – Preparation, structure and properties of $La_{0.67}Pb_{0.33}(Mn_{1-x}Co_x)O_{3-\delta}$, *Appl. Phys. A* **90** (2008) 359-365.
8. Young S. L., Chen Y. C., Chen H. Z., Hông L., and Hsueh J. F. – Effect of the substitutions of Ni^{3+} , Co^{3+} , and Fe^{3+} for Mn^{3+} on the ferromagnetic state of the $La_{0.7}Pb_{0.3}MnO_3$ manganite, *J. Appl. Phys.* **91** (2002) 8915-8917.
9. Young S. L., Chen H. Z., Lin C. C., Shi J. B., Horng L., and Shih Y. T. – Magnetotransport properties of $(La_{0.7}Pb_{0.3}MnO_3)_{1-x}Ag_x$ composites, *J. Magn. Magn. Mater.* **303** (2006) 325-328.
10. Rodriguez-Martinez L. M., and Attfield J. P. – Cation disorder and the metal-insulator transition temperature in manganese oxide perovskites, *Phys. Rev. B* **54** (1996) R15622-15625.
11. Rodriguez-Carvajal J. – Recent advances in magnetic structure determination by neutron powder diffraction, *Physica B* **192** (1993) 55-69.
12. Zlokazov V. B., and Chernyshev V. V. – MRJA - a program for a full profile analysis of powder multiphase neutron-diffraction time-of-flight (direct and Fourier) spectra, *J. Appl. Cryst.* **25** (1992) 447-451.
13. Balzar D. – Voigt-function model in diffraction line-broadening analysis, (n.d.),

- International Union of Crystallography, 1999.
14. McCusker L. B., Von Dreele R. B., Cox D. E., Louër D., and Scardi P. – Rietveld refinement guidelines, *J. Appl. Cryst.* **32** (1999) 36-50.
 15. Loan T.T., Kraus M. L. Bobrikov I. A., Vu. V. K., and Balagurov A. M. – Atomic structure of $La_{2/3}Pb_{1/3}Mn_{1-x}Co_xO_3$, *Proceedings of the 16th Conference of Young Scientists and Specialists*, Dubna, Russia (2011) 212-215.
 16. Dhahri N., Dhahri A., Cherif K. Dhahri J., Taibi K., and Dhahri E. – Structural, magnetic and electrical properties of $La_{0.67}Pb_{0.33}Mn_{1-x}Co_xO_3$ ($0 \leq x \leq 0.3$), *J. Alloys and Compounds* **496** (2010) 69-74.
 17. Troyanchuk I. O., Bushinsky M. V., Szymczak H., Barner K., and Maignan A. – Magnetic interaction in Mg, Ti, Nb doped manganites, *Eur. Phys. J. B* **28** (2002) 75-80.
 18. Lubinskii N. N., Bashkirov L. A., Galyas A. I., Shevchenko S. V., Petrov G. S., and Sirota I. M. – Magnetic susceptibility and effective magnetic moment of the Nd^{3+} and Co^{3+} ions in $NdCo_{1-x}Ga_xO_3$, *Inorganic Mater.* **44** (2008) 1015-1021.

TÓM TẮT

NGHIÊN CỨU VỀ CẤU TRÚC NGUYÊN TỬ VÀ CẤU TRÚC TỪ CỦA $La_{2/3}Pb_{1/3}Mn_{1-x}Co_xO_3$ BẰNG PHƯƠNG PHÁP NHIỀU XẠ NEUTRON VÀ SYNCHROTRON

Tô Thanh Loan^{1,*}, Bobrikov I. V.², Trần Thị Việt Nga¹, Vũ Văn Khải³, Nguyễn Huy Sinh⁴

¹*Viện ITIMS, Trường Đại học Bách khoa Hà Nội, Số 1, Đại Cồ Việt, Hà Nội*

²*Viện JINR, Số 6 Joliot-Curie, Dubna, Liên Bang Nga*

³*Trường Đại học Xây dựng, Số 55, Giải Phóng, Hà Nội*

⁴*Trường Đại học Sư phạm Kỹ thuật Hưng Yên, Khoái Châu, Hưng Yên*

*Email: totloan@itims.edu.vn

Hệ mẫu manganite pha tạp với thành phần danh định là $La_{2/3}Pb_{1/3}Mn_{1-x}Co_xO_3$ (trong đó $x = 0; 0,15, 0,20$ và $0,25$) được chế tạo bằng phương pháp phản ứng pha rắn. Cấu trúc nguyên tử, cấu trúc vi mô và cấu trúc từ của các hợp chất được nghiên cứu chi tiết sử dụng kết hợp hai phương pháp nhiễu xạ – neutron và synchrotron. Kết quả thu được chỉ ra rằng trong khoảng nhiệt độ từ 8-300 K các mẫu đều có cấu trúc trục thoi thuộc nhóm không gian $R-3c$ với các thông số mạng và khoảng cách Mn/Co-O rất đặc trưng. Các thông số vi cấu trúc thay đổi không đáng kể khi nồng độ pha tạp Co thay đổi. Trật tự từ được xác định là sắt từ và không phụ thuộc vào nồng độ Co. Giá trị mômen từ trung bình ở vị trí B vào khoảng $3,5 \mu_B$ tại vùng nhiệt độ $T < 20$ K. Quan sát được sự tồn tại của hai pha tinh thể có cùng nhóm đối xứng trong hợp chất có nồng độ pha tạp $x = 0,15$.

Từ khóa: perovskite, cấu trúc nguyên tử, cấu trúc từ, nhiễu xạ neutron, nhiễu xạ synchrotron.